Steel and Composite Structures, *Vol. 18, No. 6 (2015) 1569-1582*
DOI: http://dx.doi.org/10.12989/scs.2015.18.6.1569

Mid-length lateral deflection of cyclically-loaded braces

Therese Sheehan [*1], Tak-Ming Chan [2] and Dennis Lam [1,2]

[1] *School of Engineering and Informatics, University of Bradford, Richmond Road, Bradford BD7 1DP, United Kingdom*
[2] *Department of Civil and Environmental Engineering, The Hong Kong Polytechnic University, Hung Hom, Kowloon, Hong Kong*

(*Received May 21, 2014, Revised November 26, 2014, Accepted December 17, 2014*)

Abstract. This study explores the lateral deflections of diagonal braces in concentrically-braced earthquake-resisting frames. The performance of this widely-used system is often compromised by the flexural buckling of slender braces in compression. In addition to reducing the compressive resistance, buckling may also cause these members to undergo sizeable lateral deflections which could damage surrounding structural components. Different approaches have been used in the past to predict the mid-length lateral deflections of cyclically loaded steel braces based on their theoretical deformed geometry or by using experimental data. Expressions have been proposed relating the mid-length lateral deflection to the axial displacement ductility of the member. Recent experiments were conducted on hollow and concrete-filled circular hollow section (CHS) braces of different lengths under cyclic loading. Very slender, concrete-filled tubular braces exhibited a highly ductile response, undergoing large axial displacements prior to failure. The presence of concrete infill did not influence the magnitude of lateral deflection in relation to the axial displacement, but did increase the number of cycles endured and the maximum axial displacement achieved. The corresponding lateral deflections exceeded the deflections observed in the majority of the previous experiments that were considered. Consequently, predictive expressions from previous research did not accurately predict the mid-height lateral deflections of these CHS members. Mid-length lateral deflections were found to be influenced by the member non-dimensional slenderness ($\overline{\lambda}$) and hence a new expression was proposed for the lateral deflection in terms of member slenderness and axial displacement ductility.

Keywords: cyclic loading; concentrically-braced frames; tubular structures; concrete-filled tubes; earthquake-resisting buildings

1. Introduction

Earthquake-resisting structures employ a wide range of structural systems to ensure lateral stability under seismic actions. Diagonal braces are a popular choice owing to simplicity of design, with steel members providing a favourable strength-to-weight ratio. In recent years, attention has increasingly been paid to using concrete-filled tubular braces in these applications. Despite increasing the weight of the members, the use of concrete infill has been proved to be highly advantageous in enhancing the strength and ductility of braces. Previous research on hollow and

*Corresponding author, Ph.D., E-mail: t.sheehan@bradford.ac.uk

http://www.techno-press.org/?journal=scs&subpage=8 ISSN: 1229-9367 (Print), 1598-6233 (Online)

concrete-filled tubular braces (Elchalakani *et al*. 2003, Broderick *et al*. 2005, Sheehan and Chan 2014) has mainly focussed on the axial displacement behaviour and the number of cycles endured prior to failure. Under axial compression, slender braces exhibit flexural buckling, which can lead to excessive lateral deflections at the brace mid-height. This could potentially damage surrounding structural elements, an issue that was highlighted by Tremblay (2002) and Shaback and Brown (2003). Predictive expressions were developed theoretically by Tremblay (2002) for the mid-height lateral deflections of cyclically loaded braces covering a wide range of cross-section shapes, based on the member geometry. Two predictions were formed based on the idealised behaviour anticipated during the early stages of the test and at the end of the test. Shaback and Brown (2003) noted that actual specimen response would lie between these two cases and empirically derived an expression using test results from square hollow section (SHS) braces.

In both studies by Tremblay (2002) and Shaback and Brown (2003), the axial displacement was the main parameter found to influence the lateral deflection. Research by Broderick *et al*. (2005) and Nip *et al*. (2010) on square hollow section (SHS) and rectangular hollow section (RHS) braces under cyclic loading demonstrated that the axial displacement achieved with respect to the brace length increased as the non-dimensional global slenderness ($\overline{\lambda}$) of the brace increased. Furthermore, recent experiments carried out by Sheehan and Chan (2014) for hollow and concrete-filled circular hollow section (CHS) braces under cyclic axial loading demonstrated the improvements to performance achieved by the use of concrete infill. The CHS members tested by Sheehan and Chan (2014) had a large range of $\overline{\lambda}$ values (0.78-2.02), and the high $\overline{\lambda}$ values combined with the use of concrete infill led to considerable lateral deflections at the mid-height, exceeding the majority of lateral deflection values observed in previous tests. These findings indicated the need to explore the lateral deflection characteristics of very ductile and slender members in more detail, to ensure their safe usage in the design of earthquake-resisting buildings.

2. Experimental set-up

2.1 Specimens

Table 1 CHS specimens tested by Sheehan and Chan (2014)

Specimen ID	$\overline{\lambda}$
HF-H-1500	0.78
CF-H-1500	0.90
HF-F1-1500	0.81
HF-F2-1500	0.81
CF-F1-1500	0.92
CF-F2-1500	0.92
HF-H-3000	1.72
CF-H-3000	1.98
HF-F1-3000	1.78
HF-F2-3000	1.78
CF-F1-3000	2.02
CF-F2-3000	2.02

Experiments were carried out by Sheehan and Chan (2014) involving twelve circular hollow section braces, six of which were hot-finished and six of which were cold-formed. Both hollow and concrete-filled braces were tested for each cross-section type, and two member lengths were considered, 1,500 mm and 3,000 mm, to give non-dimensional global slenderness ($\bar{\lambda}$) values of approximately 1.0 and 2.0 in accordance with EN 1993-1-1 (2005). Table 1 presents the identification of each specimen and the non-dimensional global slenderness. The specimen name consists of 3 parts: the first part refers to manufacturing method, where "HF" denotes hot-finished and "CF" denotes cold-formed; the second part indicates whether the specimen is hollow (H) or concrete-filled (F) and the third part of the name describes the specimen length in millimetres.

The same target concrete-strength (minimum Grade C20/25 in accordance with EN 1992-1-1 (2004)) was used for all of the concrete-filled braces. All hot-finished braces had nominal dimensions of 48.3 mm (outer diameter) × 3.2 mm (tube wall thickness) and cold-formed tubes had nominal dimensions of 48.3 mm (outer diameter) × 3.0 mm (tube wall thickness). Both cross-section types were Class 1 in accordance with EN 1993-1-1 (2005).

2.2 Test procedure

The braces were subjected to the cyclic axial loading protocol outlined in the ECCS guidelines (ECCS 1986) consisting of equal axial displacements in compression and tension. Axial displacement amplitudes were defined by the yield displacement $\delta_y = f_y L/E$, where f_y was the yield strength of the material, L was the brace length and E was the modulus of elasticity. The first four cycles consisted of displacement amplitudes of $0.25\delta_y$, $0.50\delta_y$, $0.75\delta_y$ and $1.0\delta_y$ in both compression and tension, followed by three cycles at amplitudes of $2\delta_y$, $4\delta_y$, $6\delta_y$, etc. until the specimen failed. Braces were tested in a purpose-built test-rig as shown in Fig. 1(a). Mid-height lateral deflections were measured in the plane of the frame and in the orthogonal direction using calibrated string potentiometers. The specimens were welded onto thick end plates, with a pair of stiffeners at each end, and the plates were then bolted into the test-rig. The stiffeners were used to

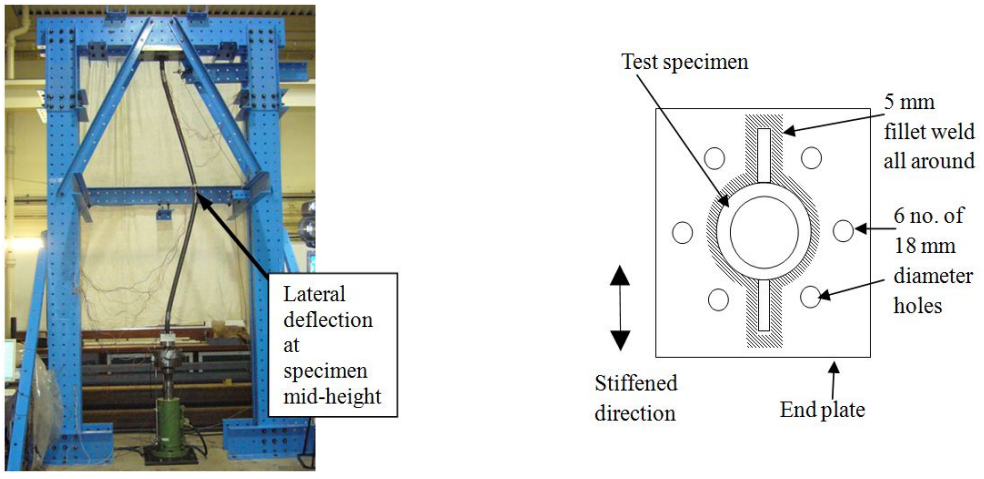

(a) Test-rig (b) Specimen end details (plan view)

Fig. 1 Testing arrangements for CHS braces

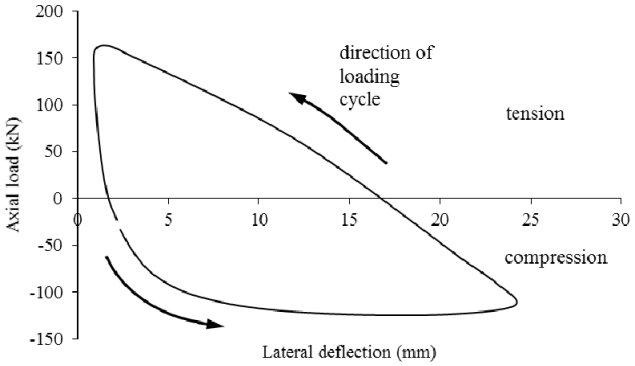

Fig. 2 Relationship between axial load and lateral deflection for a typical loading cycle

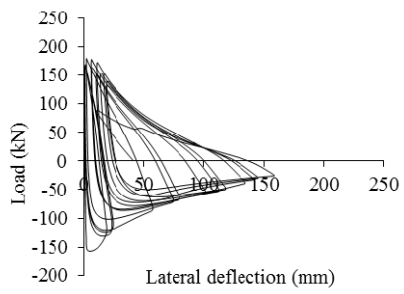

(a) Specimen HF-H-1500

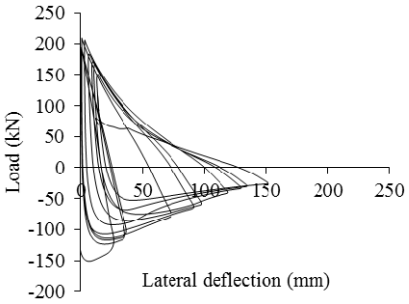

(b) Specimen CF-H-1500

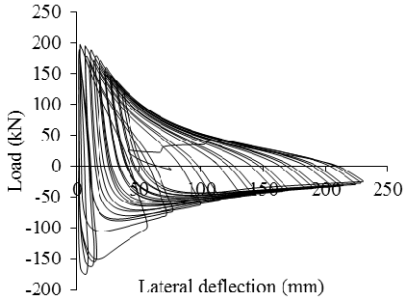

(c) Specimen HF-F1-1500

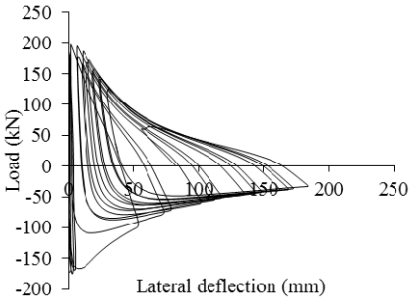

(d) Specimen HF-F2-1500

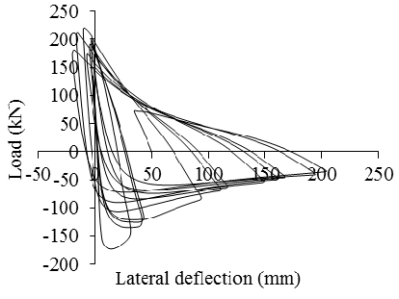

(e) Specimen CF-F1-1500

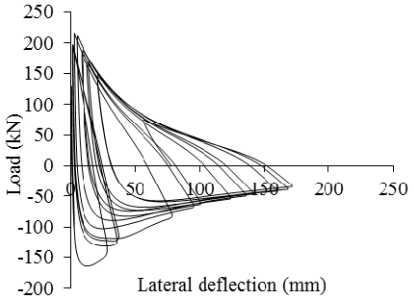

(f) Specimen CF-F2-1500

Fig. 3 Axial load versus mid-height lateral deflection for 1,500 mm specimens

ensure the integrity of the welded connections and to control the direction of flexural buckling of the member. A plan view of the specimen end arrangement is presented in Fig. 1(b). The end conditions were assumed to be restrained against rotation and the effective length of the braces was assumed to be 0.7 L. This was slightly larger than the theoretical value 0.5 L but took into account the imperfections in the test set-up, such as flexibility of the test-rig and misalignment of the specimen ends.

2.3 Test results

Flexural buckling occurred at an early stage of each test, after which lateral deflections became more pronounced with increasing axial displacement. The tests were terminated after local buckling and fracture occurred at the mid-height or ends. Fig. 2 shows the relationship between axial load and lateral deflection for a single cycle of a typical test. The mid-height lateral deflection increased slowly at the beginning of the first half-cycle (compression), and then more rapidly after the occurrence of flexural buckling. In the second half of the cycle (tension), the lateral deflection decreased rapidly with respect to the change in load, as the member was straightened.

Fig. 3(a)-(f) shows the complete axial load-lateral deflection relationships for each of the 1,500 mm braces. As Fig. 3 demonstrates, the presence of concrete infill did not significantly influence the magnitude of lateral deflections, or the shapes of the curves. Similarly, axial load-lateral deflection relationships are presented for each of the 3,000 mm long braces in Fig. 4(a)-(f). Again, the presence of concrete infill did not have a noticeable influence on the lateral deflection behaviour of the braces. However, the shapes of the curves for the 3,000 mm braces were distinct from those of the 1,500 mm braces. The curves for the longer braces enclosed a smaller area than those of the shorter braces, and exhibited a sharper increase in load during the tensile half of each cycle. Overall, some similarities were also observed between the specimen lengths. In all cases, the braces became less stiff as the loading protocol progressed, causing the lateral deflections to increase and the buckling load to decrease with each progressive cycle. As the members became elongated, there was a residual lateral deflection at the point of zero load when reversing from compression into tension and this increased with each cycle.

The development of lateral deflection with increasing axial displacement, δ, is shown for the 1st, 2nd and 3rd cycles at each axial displacement amplitude in Figs. 5(a) and (b) for hot-finished specimens HF-H-1500 and HF-H-3000 respectively. Here, δ is normalized with respect to δ_y. The lateral deflection increased significantly between the 1st and 2nd cycles at each amplitude, owing to the elongation of the specimen in tension, but there was little difference between the lateral deflections that occurred in the 2nd and 3rd cycles. Similar trends were observed for the concrete-filled and cold-formed braces.

In most cases, the lateral deflections were predominantly in the “unstiffened” direction (Fig. 1(b)). For the 3,000 mm cold-formed braces however, deflections occurred at an angle between the stiffened and unstiffened directions, and hence the resultant deflection magnitude was used. The direction of the deflection may have been due to out-of-roundness of the cross-section or the seam-weld position but this could not be confirmed without further experiments.

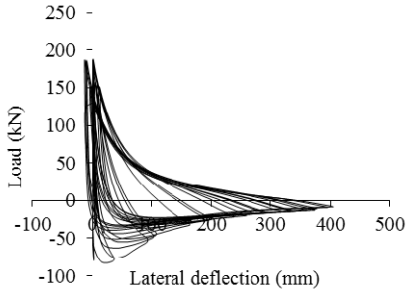

(a) Specimen HF-H-3000

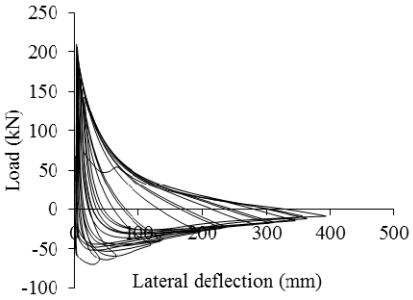

(b) Specimen CF-H-3000

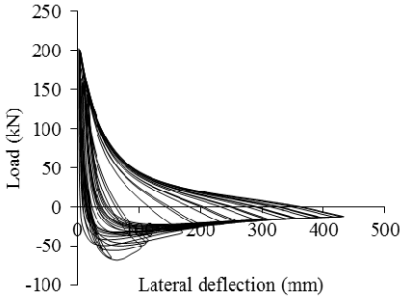

(c) Specimen HF-F1-3000

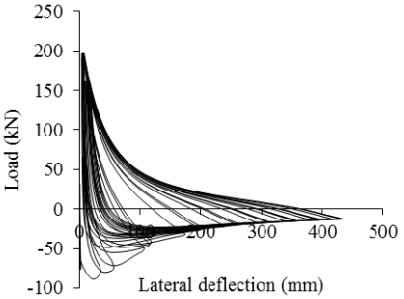

(d) Specimen HF-F2-3000

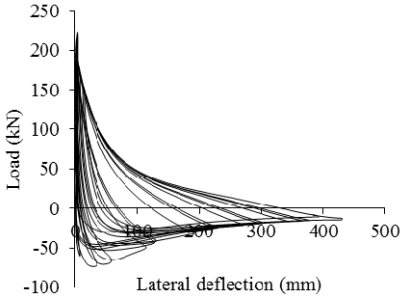

(e) Specimen CF-F1-3000

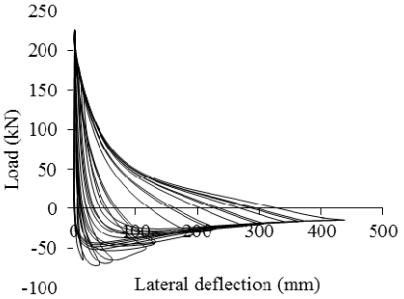

(f) Specimen CF-F2-3000

Fig. 4 Axial load versus mid-height lateral deflection for 3,000 mm specimens

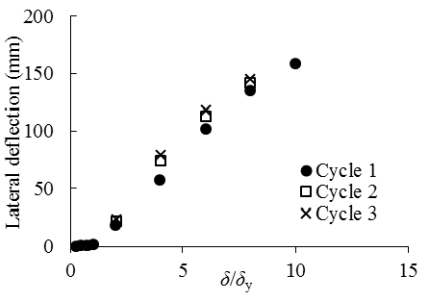

(a) HF-H-1500

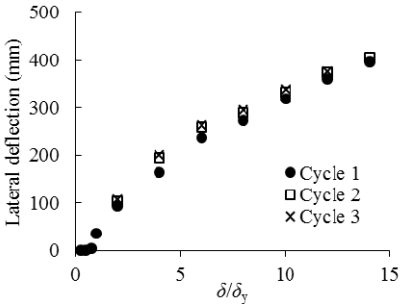

(b) HF-H-3000

Fig. 5 Lateral deflection at 1st, 2nd and 3rd cycles of each displacement amplitude

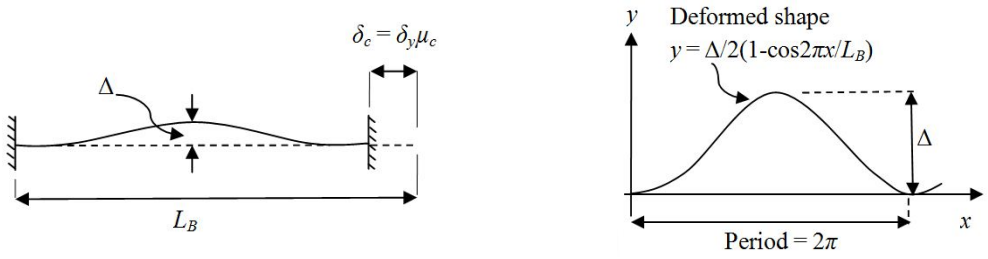

(a) Deformation of brace under elastic buckling (b) Sinusoidal wave function

Fig. 6 Deformed shape of brace under elastic buckling

3. Predictive expressions

3.1 Previous predictions for lateral deflections

Expressions were proposed by Tremblay (2002) for predicting the mid-height lateral deflections considering two different scenarios:

(1) For low axial displacements where the brace underwent elastic buckling
(2) For high axial displacements where the response was a plastic mechanism.

For the first case, the deformed shape was described by a sinusoidal wave function. The geometry of the deformed shape and corresponding sine wave are presented in Fig. 6.

Taking the period of the wave to be 2π, the brace length to be L_B and the amplitude to be $\Delta/2$, the deflected shape was described by

$$y = \frac{\Delta}{2}\left(1 - \cos\left(\frac{2\pi x}{L_B}\right)\right) \tag{1}$$

where x represented the direction along the member axis and y was the direction of the deflection. Assuming the brace to be incompressible, the compressive axial displacement, δ_c was expressed as

$$\delta_c = \int_0^{L_B} \frac{1}{2}\left(\frac{dy}{dx}\right)^2 dx \tag{2}$$

Obtaining dy/dx from Eq. (1) and integrating Eq. (2) led to the following equation for the lateral deflection of braces under low axial displacements

$$\Delta = \frac{2}{\pi}\sqrt{\delta_c L_B} \tag{3}$$

The second case considered was for members forming a plastic mechanism, with plastic hinges at the mid-length and specimen ends, with the brace remaining straight in between the hinges. The geometry is shown in Fig. 7. L_H referred to the distance between the plastic hinges near the brace ends, which were assumed to occur at a distance equal to the cross-section diameter from the end of the brace.

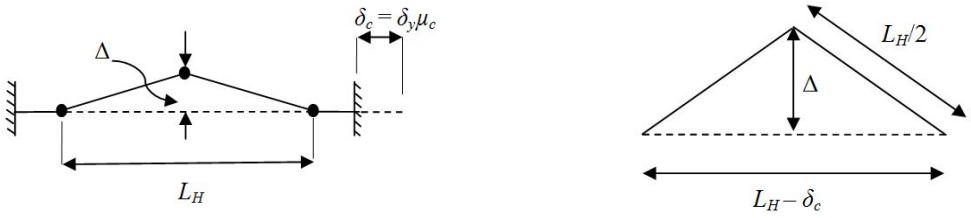

(a) Deformation of brace forming plastic mechanism (b) Assumed geometry

Fig. 7 Deformed shape and assumed geometry for brace forming plastic mechanism

The lateral deflection Δ was related to δ_c and L_H using Pythagoras' theorem and the geometry of Fig. 7(b). Since the value of δ_c was considerably smaller than L_H, the δ_c^2 was omitted to give the following expression.

$$\Delta = \frac{1}{\sqrt{2}}\sqrt{\delta_c L_H} \tag{4}$$

Eqs. (3) and (4) did not take into account the permanent axial deformation resulting from the previous cycles and hence Tremblay (2002) modified these as follows

$$\Delta = \frac{2}{\pi}\sqrt{(\mu_c + \mu_t - 1)\delta_y L_B} \tag{5}$$

$$\Delta = \frac{1}{\sqrt{2}}\sqrt{(\mu_c + \mu_t - 1)\delta_y L_H} \tag{6}$$

where μ_c and μ_t refer to the compressive displacement ductility of the cycle in question (δ/δ_y) and the tensile displacement ductility of the previous half-cycle respectively. Eqs. (5) and (6) were developed by Tremblay (2002) considering two extreme cases: braces under very low axial displacements and braces under very high axial displacements, which may be observed near the very beginning and end of the test. However, not all specimens can achieve the plastic mechanism considered in Eq. (6) before failure. In reality, braces are mostly expected to exhibit behaviour that lies between each of these two cases. This was considered by Shaback and Brown (2003), who derived an expression empirically using data from square hollow section (SHS) bracing tests, given as

$$\frac{\Delta}{L}(\%) = -0.11(\mu)^{1.9} + 2\mu \tag{7}$$

The lateral deflection in Eq. (7) was related to the displacement ductility ($\mu = \delta/\delta_y$). The CHS tested by Sheehan and Chan (2014) were found to obtain higher axial displacements prior to failure than the RHS specimens of Shaback and Brown (2003) and hence a new set of expressions was proposed to take account of the response under higher axial displacements. Separate equations were developed for hot-finished and cold-formed braces and these are presented by Eqs. (8) and (9) respectively.

$$\frac{\Delta}{L}(\%) = -0.05\mu^2 + 1.88\mu - 0.41 \tag{8}$$

$$\frac{\Delta}{L}(\%) = -0.15\mu^2 + 3.10\mu - 1.60 \tag{9}$$

3.2 Comparison between experimental data and previous predictions

Figs. 8 and 9 compare the mid-height lateral deflections obtained in the CHS experiments (Sheehan and Chan 2014) with the previous predictions (Tremblay 2002, Shaback and Brown 2003) and those of Eqs. (8) and (9) for hot-finished and cold-formed braces respectively.

For hot-finished 1,500 mm braces, the predictions of Shaback and Brown (2003) (Eq. (7)) overestimated the lateral deflections (Δ) under low axial displacements and underestimated the deflections for values of axial displacement/length (δ/L) that were greater than 0.01. Eq. (7) also underestimated the deflections of 3,000 mm specimens for the entire range of axial displacements considered. The noticeable deviation under higher axial displacements ($\delta/L > 0.025$) suggests that the specimens used by Shaback and Brown (2003) to develop Eq. (7) did not achieve δ values in this range prior to failure. The 'plastic' mechanism case proposed by Tremblay (2002) (Eq. (6))

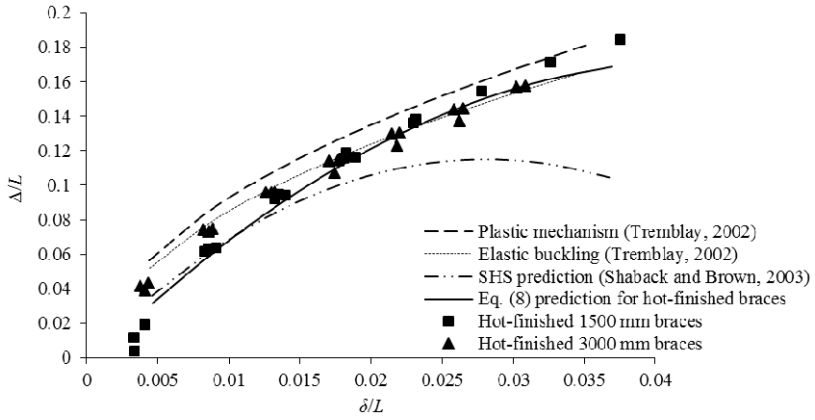

Fig. 8 Lateral deflections for hot-finished specimens in the 3rd cycle of each displacement amplitude

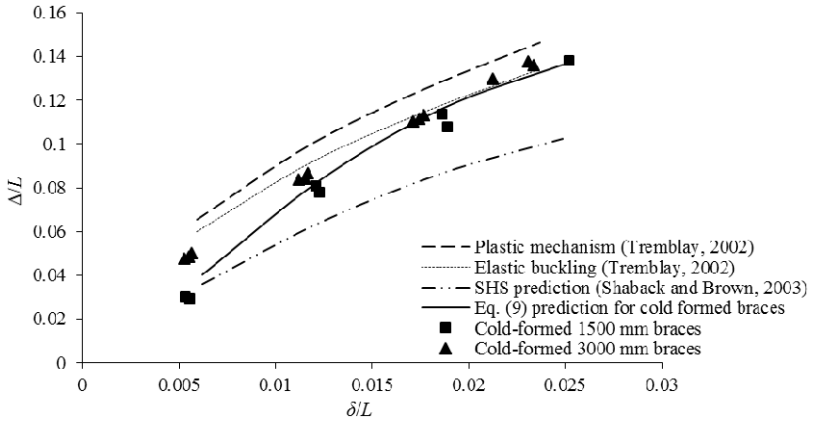

Fig. 9 Lateral deflections for cold-formed specimens in the 3rd cycle of each displacement amplitude

overestimated the lateral deflection in all cases and hence provided a suitable upper bound to the test data. Although the actual lateral deflections were significantly smaller than the Eq. (6) predictions under low values of axial displacement, the data points approached this upper bound in the later stages of the test, as the plastic hinges developed. Ideally, the 'elastic' case proposed by Tremblay (2002) (Eq. (5)) should have produced a lower bound to the predicted lateral deflections, but in reality this also tended to overestimate the lateral deflection for δ/L values less than 0.02. As stated by Tremblay (2002), the 'elastic' case did not take into consideration the elastic axial shortening of the member in compression, but it was found that including this made little difference to the predictions. Similar trends were observed between the cold formed specimen data in Fig. 9 and the predictions of Tremblay (2002) and Shaback and Brown (2003). Eq. (7) underestimated the lateral deflection in all cases except for the 1,500 mm braces under low axial displacements ($\delta/L < 0.01$). Eq. (5) overestimated the lateral deflection for $\delta/L < 0.02$ and underestimated the deflection in the lateral stages of the test, whereas Eq. (6) overestimated the mid-length lateral deflection for all braces at all stages of the test. The predictions of Eqs. (8) and (9) for hot-finished and cold formed braces provided a reasonable overall fit to the experimental data for low and high axial displacements. However, under low axial displacements, the 3,000 mm braces underwent noticeably larger lateral deflections in relation to their length than the 1,500 mm specimens. Eqs. (8) and (9) only provided a 'best-fit' between the data points in this range, without showing a very close correlation to the data of either specimen-length. The difference in behaviour between 1,500 mm and 3,000 mm specimens is also apparent in the axial load-lateral deflection relationships that are presented in Figs. 3 and 4. These observations suggest that a better agreement may be obtained by relating the mid-height lateral deflection to the non-dimensional global slenderness, $\overline{\lambda}$.

3.3 Prediction for lateral deflections using global slenderness

As discussed by Tremblay (2002) and Shaback and Brown (2003) the lateral deflection is mainly influenced by the axial displacement of the brace, and for the purpose of design, previous researchers have developed predictive expressions for the lateral deflection in terms of axial displacement ductility, μ. The differences between Figs. 3 and 4 and the observations of Figs. 8 and 9 also suggest that the non-dimensional slenderness, $\overline{\lambda}$, has an effect on the behaviour. A regression analysis was carried out using the test data of Sheehan and Chan (2014) to assess the influence of μ and $\overline{\lambda}$ on Δ. Equations were developed for the relationship between the three parameters considering different orders of μ. Although Eqs. (7)-(9) employed μ^2 and $\mu^{1.9}$ terms, $\sqrt{\mu}$ was found to have a greater effect on Δ and hence Eq. (10) was proposed for braces of all cross-section types

$$\frac{\Delta}{L}(\%) = 7.6\sqrt{\mu} - 1.5\overline{\lambda}\sqrt{\mu} + 4.2\overline{\lambda} - 9.5 \tag{10}$$

This single expression was proposed for hollow and concrete-filled hot-finished and cold-formed braces and was examined for a wider range of test data from Shaback and Brown (2003), Nip *et al*. (2010) and Fell (2008) in addition to the data of Sheehan and Chan (2014), to take into account different cross-section types and slenderness ranges. Table 2 summarises the specimens that were employed from each study, indicating the cross-section type (forming process, steel type, shape), cross-section dimensions and non-dimensional global slenderness, $\overline{\lambda}$. All cross sections were tubular and had a cross-section classification of Class 1 in accordance with EN

Table 2 Test data for cyclic braces

Reference	Specimen name	Specimen type	Cross-section dimensions (mm) (width × depth × thickness)	$\overline{\lambda}$
Shaback and Brown (2003)	1B	Cold-formed carbon steel SHS	127 × 127 × 8.0	0.81
	2A		152 × 152 × 8.0	0.79
	2B		152 × 152 × 9.5	0.79
	3A		127 × 127 × 6.4	1.00
	3B		127 × 127 × 8.0	0.98
	3C		127 × 127 × 9.5	0.94
	4A		152 × 152 × 8.0	0.95
	4B		152 × 152 × 9.5	0.90
Nip *et al*. (2010)	60 × 40 × 3 × 1250-SS-CF	Cold-formed stainless steel RHS	60 × 40 × 3	0.54
	60 × 40 × 3 × 2050-SS-CF		60 × 40 × 3	0.97
	60 × 40 × 3 × 2850-SS-CF		60 × 40 × 3	1.40
	40 × 40 × 3 × 1250-CS-HR	Hot-finished carbon steel SHS	40 × 40 × 3	0.50
	40 × 40 × 3 × 1250-CS-CF	Cold-formed carbon steel SHS	40 × 40 × 3	0.50
	50 × 50 × 3 × 1250-SS-CF	Cold-formed stainless steel SHS	50 × 50 × 3	0.45
Fell (2008)	HSS1-1	Cold-formed carbon steel SHS	101.6 × 101.6 × 6.4	1.15

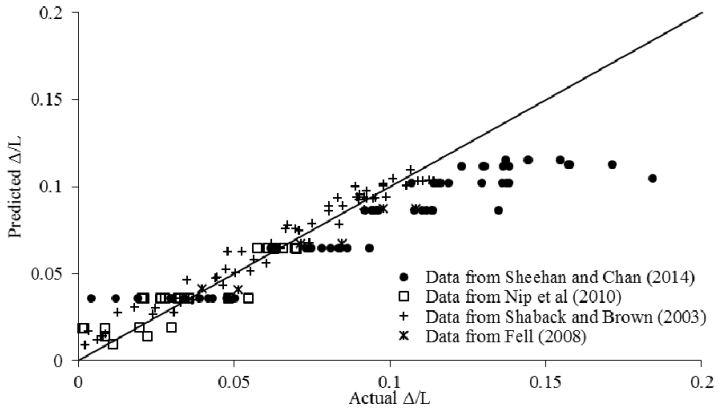

Fig. 10 Comparison between predicted lateral deflection using Eq. (7) (Shaback and Brown 2003) and actual lateral deflection measured during experiments

1993-1-1 (2005). Cross-sections of other types/classifications were not included in this comparison, mainly due to the absence of available experimental data. Hence these will need to be considered

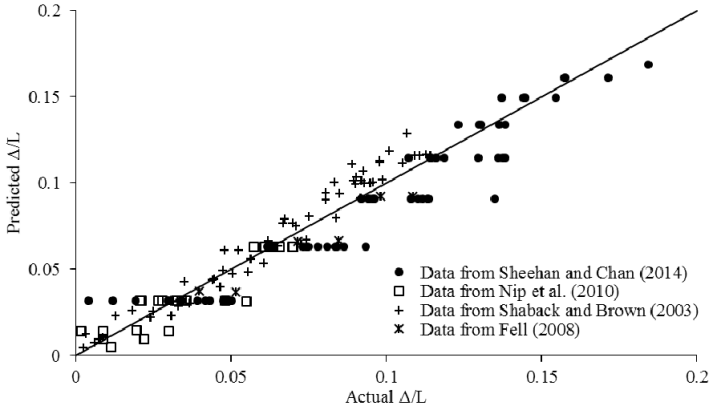

Fig. 11 Comparison between predicted lateral deflection using Eq. (8) and actual lateral deflection measured during experiments

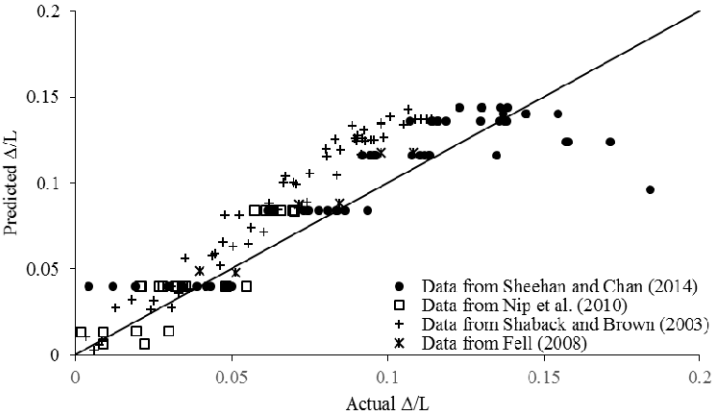

Fig. 12 Comparison between predicted lateral deflection using Eq. (9) and actual lateral deflection measured during experiments

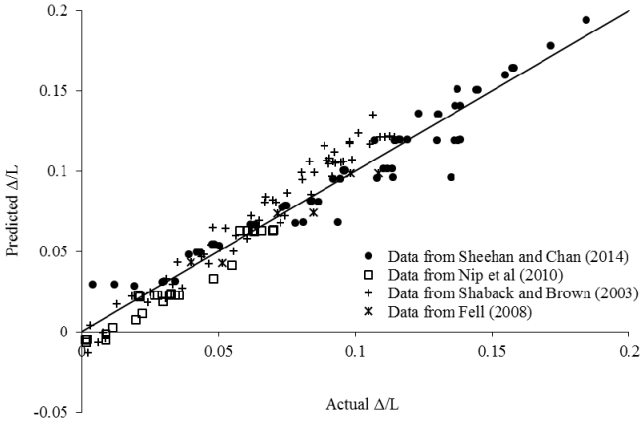

Fig. 13 Comparison between predicted lateral deflection using Eq. (10) and actual lateral deflection measured during experiments

Table 3 Reliability of predictions for Eqs (7)-(10)

Eq. No.	Reference	R^2	COV
(7)	Shaback and Brown (2003)	0.893	0.250
(8)	Current study	0.922	0.164
(9)	Current study	0.832	0.255
(10)	Current study	0.942	0.148

in future work.

Figs. 10-13 compare the accuracy of Eqs. (7)-(10) for the specimens in Tables 1 and 2. Eq. (7) provides reasonable predictions for Δ/L values less than 0.10 but shows considerable discrepancies for higher values of Δ/L. Eq. (8) shows a more even correlation across all ranges of Δ/L but there are still significant differences in many cases between the predicted and actual lateral deflections. Eq. (9) overpredicts the lateral deflections for Δ/L values in the range of 0.05-0.13 and underpredicts the lateral deflections for higher Δ/L values. Overall Eq. (10) provides more reliable predictions than Eqs. (7)-(9) across all values of lateral and axial displacement, confirming that global slenderness $\bar{\lambda}$ is one of the main indicators of lateral deflection behaviour for cyclically loaded braces.

The R^2 and coefficient of variation (COV) for Eqs. (7)-(10) are presented in Table 3. Eq. (10) proposed in this paper has the largest R^2 value (0.942) and smallest COV (0.148) confirming that Eq. (10) provides the most reliable prediction of mid-height lateral deflection for cyclically loaded braces. This has been verified for members covering a wide range of global slenderness values ($\bar{\lambda}$ = 0.5-2.0) but for a smaller range of cross-section types (Class 1 tubular sections only). Hence further work will be needed to assess the expression for other cross-sections. To avoid the time and costs associated with experiments, this may be achieved using a numerical approach such as finite element modelling.

4. Conclusions

This study examined the lateral deflections at the mid-height for hollow and concrete-filled hot-finished and cold-formed braces under cyclic axial loading. The following conclusions were drawn:

- The presence of concrete infill did not affect the relationship between lateral deflection and axial displacement of CHS braces. However, concrete-filled braces endured larger axial displacements than their hollow counterparts and hence exhibited larger axial deflections.
- Predictions by Tremblay (2002) and Shaback and Brown (2003) tended to overestimate or underestimate the mid-height lateral deflection of circular hollow section braces.
- Predictions formulated by Eqs. (8) and (9) provided a reasonable overall average fit to the lateral deflection data for braces of different global slenderness values but were less accurate for low axial displacements.
- Mid-length lateral deflections are related to the member slenderness in addition to the displacement ductility. Reliable predictions were formulated for the lateral deflections using these two parameters.

- The proposed equations have been verified using mostly data from circular and square tubular braces, with cross-section classifications of Class 1 in accordance with EN 1993-1-1 (2005). Therefore they may not be as reliable for cross-sections of other classifications.
- The results may be extended in future by conducting finite element analysis on a wider range of section types and sizes.

Acknowledgments

The authors gratefully acknowledge the financial support from Tata Steel for the experiments and for the technical assistance provided by the laboratories and workshops in the School of Engineering, The University of Warwick.

References

Broderick, B.M., Goggins, J.M. and Elghazouli, A.Y. (2005), "Cyclic performance of steel and composite bracing members", *J. Construct. Steel Res.*, **61**(4), 493-514.

ECCS (1986), Recommended Testing Procedure for Assessing the Behaviour of Structural Steel Elements under Cyclic Loads; European Convention for Constructional Steelwork, Brussels, Belgium.

Elchalakani, M., Zhao, X.L. and Grzebieta, R. (2003), "Tests of cold formed circular tubular braces under cyclic axial loading", *J. Struct. Eng.*, **129**(4), 507-514.

EN 1992-1-1 (2004), Design of concrete structures, Part 1-1: General rules and rules for buildings; European Standard, CEN, Brussels, Belgium.

EN 1993-1-1 (2005), Design of steel structures, Part 1-1: General rules and rules for buildings; European Standard, CEN, Brussels, Belgium.

Fell, B.V. (2008), "Large-scale testing and simulation of earthquake-induced ultra low cycle fatigue in bracing members subjected to cyclic inelastic buckling", Ph.D. Thesis; University of California, Davis, CA, USA.

Nip, K.H., Gardner, L. and Elghazouli, A.Y. (2010), "Cyclic testing and numerical modelling of carbon steel and stainless steel tubular bracing members", *Eng. Struct.*, **32**(2), 424-441.

Shaback, B. and Brown, T. (2003), "Behaviour of square hollow structural steel braces with end connections under reversed cyclic axial loading", *Can. J. Civil Eng.*, **30**(4), 745-753.

Sheehan, T. and Chan, T.M. (2014), "Cyclic response of hollow and concrete-filled CHS braces", *Proceedings of the ICE – Structures and Buildings*, **167**(3), 140-152.
DOI: http://dx.doi.org/10.1680/stbu.12.00033

Tremblay, R. (2002), "Inelastic seismic response of steel bracing members", *J. Construct. Steel Res.*, **58**(5-8), 665-701.

CC